

TURBULENT TRANSPORTS MODELING IN A HYDROGEN-AIR DIFFUSION FLAME

Sylvain Serra, Vincent Robin, Arnaud Mura, Michel Champion
Institut Pprime - UPR 3346 - CNRS - ENSMA - Université de Poitiers
BP 40109, 86961 Futuroscope, France
vincent.robin@ensma.fr

ABSTRACT

Turbulent transports in hydrogen-air flame are investigated by introducing relevant scalar variables which allow to identify and treat separately density effects induced by both mixing and reactive processes. The algebraic models proposed for the turbulent scalar flux and the turbulent kinetic energy allow to recover and generalise well-known previously established relations and highlight the possible occurrence of counter-gradient turbulent diffusion. The calculation of a practical turbulent diffusion hydrogen-air flame is also performed and exhibits a strong production of turbulence near stoichiometric conditions.

INTRODUCTION

Thermal expansion in reactive flows has a strong effect on turbulent transports as shown in the pioneering studies conducted by Bray *et al.* (1981), Libby & Bray (1981), and Borghi & Escudé (1984). It is now well established that the large density variations involved in these fully premixed flames lead to counter-gradient turbulent diffusion and flame generated turbulence phenomena. However, the behaviour of turbulent transports in diffusion flames, which can be described by using passive scalars, such as the Schvab-Zel'dovich variable or the mixture fraction, is always considered identical to those observed in inert flows. This assumption is also invoked because diffusion flames differs for premixed ones which propagate and impose their own dynamics to the flow. Moreover, it is commonly considered that the key difficulty in flames is the modeling of the mean chemical rate and not the modeling of the turbulent transports. Therefore, works focusing on turbulent transports evolution in diffusion flames remain very scarce, see for example, Stårner & Bilger (1981), Stårner (1983), Luo & Bray (1998).

Our point of view is that the mean chemical rate and turbulent transports are strongly correlated and cannot be modeled separately. Moreover, counter gradient turbulent diffusion has been evidenced in non premixed flames from the experiments of Hardalupas *et al.* (1996) but also from the direct numerical simulation of Luo (2000). The heat release induced density changes in such diffusion flames are of the same order of magnitude as those occurring in premixed flames. Consequently, turbulent transport must be also strongly affected by density variations since density is straightly correlated to velocity via the mass conservation

law. The density - via the equation of state - is also related to scalar quantities such as temperature or species mass fractions. Therefore, the objective of this work is to develop a new strategy to represent turbulent transports, i.e. scalar flux and turbulent kinetic energy, in non-premixed reactive flows featuring large density variations. This study focuses on the very specific and complicated case of hydrogen-air combustion where significant density variations may be induced by both heat release due to chemical reactions and non-reactive mixing between hydrogen and air.

DENSITY VARIATIONS IN HYDROGEN-AIR FLAMES

Since density effect is the cornerstone of the present study, the most relevant scalar to deal with such flows must be directly related to density. Thus, the normalized specific volume f is introduced as a representative scalar:

$$f = (r - r_{\min})/\beta, \quad (1)$$

where $r=1/\rho$ and $\beta = (r_{\max} - r_{\min})$. The main advantage of this variable is that it can be used in premixed flames where f is the usual progress variable c of chemical reactions but can also be used in the case of passive mixing of two streams of different density where f is the usual mixture fraction ξ . Therefore, the normalized specific volume f seems appropriate to describe diffusion flames where both processes, i.e. chemical reactions and mixing, are involved. However, if chemical reactions are considered as infinitely fast when compared to mixing processes, the state of the mixture is given by the chemical equilibrium and the function $f(\xi)$ is known, see Fig. (1). Thus, the knowledge of the mixture fraction ξ , which represents the level of passive mixing between fuel and oxidizer streams, is sufficient to describe the state of the mixture in diffusion flames. Figure (1), which shows a monotonic evolution of $f(\xi)$, emphasizes the specific behaviour of hydrogen-air combustion where the variations of density associated with non reactive mixing and the effects of the heat release reach the same order of magnitude. The former effect is represented by the pure mixing line in Figure (1), which is linearly related to the mixture fraction evolution, whereas the latter effect is represented by the temperature evolution $T(\xi)$, which is a strongly non linear function of the mixture fraction. Accordingly, the potential effects of density on the velocity field is conditioned by the values of the mixture fraction. These effects may be very important around

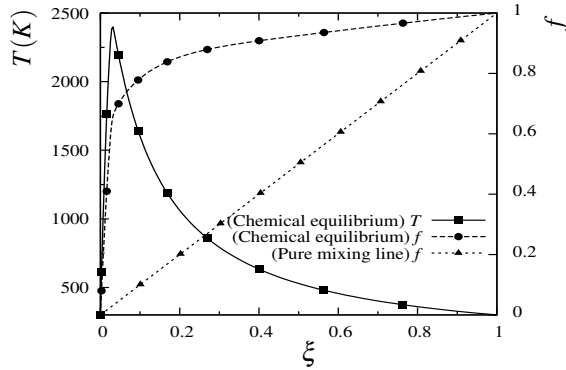


Figure 1: Chemical equilibrium profiles for temperature T and f .

stoichiometric conditions ($\xi_{st} = 2.85 \times 10^{-2}$) where $T(\xi)$ reaches a maximum.

The normalized specific volume introduced in Eq. (1) also allows to rewrite easily correlations $\overline{u''}$, $\overline{\xi''}$ and $\overline{f''}$ as follow:

$$\overline{u''} = \overline{(\rho u'' r)} = \beta \overline{\rho u'' f''}, \quad (2)$$

$$\overline{\xi''} = \overline{(\rho \xi'' r)} = \beta \overline{\rho \xi'' f''}. \quad (3)$$

$$\overline{f''} = \overline{(\rho f'' r)} = \beta \overline{\rho f''^2}. \quad (4)$$

These correlations associated with the mean pressure gradient correspond to the velocity-pressure and scalar-pressure terms of the transport equations for the Reynolds stresses $\overline{\rho u'' u''}$, the passive scalar turbulent flux $\overline{\rho u'' \xi''}$ and the reactive scalar turbulent flux $\overline{\rho u'' f''}$. These terms are known to be of first order importance and must be modelled carefully when density variations occur. Equations (2), (3) and (4) clearly show that $\overline{u''}$, $\overline{f''}$ are nothing else than the turbulent scalar flux and the variance of the normalized specific volume and $\overline{\xi''}$ is the co-variance between the normalized specific volume and the mixture fraction. Relations (2), (3) and (4) are also fully consistent with: (i) the relation previously established by Jones (1994): $\overline{u''} = \overline{\xi'' u'' \xi''} / \overline{\xi''^2}$, when non reactive mixing is considered, i.e. $f = \xi$ and (ii) the well-known relations obtained for fully premixed combustion ($f = c$): $\overline{u''} = \beta \overline{\rho u'' c''}$ and $\overline{c''} = \beta \overline{\rho c''^2}$. Therefore, the normalized specific volume f is a relevant scalar when variable density flows are considered: it can be used for both passive and reactive flows, it is able to highlight the specificity of hydrogen-air flames and it allows to recover and generalise well-known previously established relations.

VELOCITY SPLITTING PROCEDURE

In the proposed approach, the modeling of turbulent transport, i.e. passive scalar flux $\overline{\rho u'' \xi''}$ and turbulent kinetic energy $\overline{\rho u'' u''}$, consists in splitting the velocity field into two distinct contributions:

$$u = v + w, \quad (5)$$

in order to treat separately effects of turbulence and effects of density variations on the velocity field. On the one hand, the velocity variations induced by density changes are associated with the w -velocity field. On the other hand, the v -velocity field is associated with turbulent mixing effects.

Such a splitting procedure was previously applied with some success to model turbulent fluxes in premixed flames, see Robin *et al.* (2012a) and Dong *et al.* (2013). This procedure is well suited to such situations because the flame brush is considered to be composed of one dimensional premixed flamelet structures through which the acceleration is a linear function of the progress variable c . Accordingly, Robin *et al.* (2011) define the norm of the w -velocity as proportional to the progress variable: $\|w\| = \tau S_L c$, where S_L is the laminar flame propagation velocity speed, and τ is the expansion factor defined as $\tau = \rho_{\max} \beta$.

However, in non premixed reactive flows, the norm of the w -velocity cannot be considered any longer as proportional to the scalar, i.e. the mixture fraction ξ . We consider this velocity as proportional to the normalized specific volume f introduced above in order to be consistent with the previous work of Robin *et al.* (2011):

$$\|w\| = s \beta f, \quad (6)$$

where s is a constant parameter associated to a mass flow rate per unit flame area. Therefore, the previous analysis conducted for premixed situations by Robin *et al.* (2011) remains valid provided that the normalized specific volume f is considered instead of the progress variable c and the parameter s instead of $\rho_{\max} S_L$.

The splitting procedure is then applied to the scalar turbulent flux by using Eq. (5):

$$\overline{\rho u'' \xi''} = \overline{\rho v'' \xi''} + \overline{\rho w'' \xi''}, \quad (7)$$

where the scalar turbulent fluxes $\overline{\rho v'' \xi''}$ and $\overline{\rho w'' \xi''}$ are modeled following the proposal of Robin *et al.* (2012b) and applying the definition of Eq.(6), so that the formal expression of the scalar turbulent flux may be written:

$$\overline{\rho u'' \xi''} = -\overline{\rho} (v_T / \sigma_T) \nabla \xi + \overline{\rho} s \beta \lambda (1 + \psi) \overline{\xi'' f''} M. \quad (8)$$

The first term in the Right Hand Side (RHS) of Eq.(8) is associated with the passive turbulent mixing between the two reactant streams. It is represented with a gradient law. The second term of the RHS represents the *direct* and *indirect effects* of thermal expansion on the scalar turbulent flux, see Robin *et al.* (2011). The *direct effects* are induced by the local variations of density. The corresponding modeled expression involves a unit vector M that characterizes the mean orientation of the scalar flux and a parameter λ that measures the associated local fluctuations, see Robin *et al.* (2012a) for more details. The *indirect effects* correspond to the acceleration induced by the flowfield curvature. These effects have been modeled by invoking an analogy with the *direct effects* via the introduction of the model parameter ψ .

Equation (8) also involved the covariance $\overline{\xi'' f''}$ already discussed in Eq. (3). This term appears in the transport equation for the passive scalar flux $\overline{\rho u'' \xi''}$. Doing so, the behaviour of the algebraic model (8) should be similar to the one obtained by solving a transport equation for the scalar flux. Moreover, Eq.(8) involves the quantity s , analogous to a chemical consumption rate ($Kg.m^{-2}.s$). Therefore we can conclude that even if the mixture fraction is a passive scalar, the only unclosed term of its mean transport equation, i.e. $\overline{\rho u'' \xi''}$, does depend on reactive processes.

Consideration of such a splitting procedure allows the turbulent kinetic energy to be expressed as:

$$\overline{\rho k} = \overline{\rho k_{vT}} + \frac{1}{2} \overline{\rho} (s\beta)^2 (1 + \psi^2) \left[\overline{f'^2} + \tilde{f}^2 (1 - \lambda^2) \right], \quad (9)$$

where $\overline{\rho k_{vT}}$ represents the turbulent kinetic energy induced by pure mixing processes. We consider here that $\overline{\rho k_{vT}}$ can be resolved by using the same modeled transport equation as the one retained for non reactive flows. The second term of the RHS of Eq.(9) involves the parameter s and the variance of the normalized specific volume $\overline{f'^2}$ already discussed in Eq. (4).

Thus, this variance (or $\overline{f''}$) associated with the mean pressure gradient corresponds to the scalar-pressure term of the transport equation for the reactive scalar flux $\overline{\rho u'' f''}$. This scalar flux is directly related to $\overline{u''}$, see Eq. (2), and is involved in the velocity-pressure term of the transport equation for the turbulent kinetic energy $\overline{\rho k}$. Therefore, this velocity splitting procedure is fully consistent with a second order approach and able to provide algebraic closures for the turbulent transport terms, as an alternative to solving additional transport equations.

The reactive scalar flux $\overline{\rho u'' f''}$ can be modeled by employing the same strategy:

$$\overline{\rho u'' f''} = -\overline{\rho} (v_T / \sigma_T) \nabla \tilde{f} + \overline{\rho} s \beta \lambda (1 + \psi) \overline{f'^2} M. \quad (10)$$

It should be noticed that the ratio of the second terms of the RHS of the modeled passive and reactive scalar fluxes, i.e. thermal expansion terms in Eq.(8) and Eq.(10), leads to $\overline{\rho u'' f''} / \overline{\rho u'' \xi''} = \overline{f'^2} / \overline{\xi'' f''}$, which may be rewritten using Eqs. (2) and (4) as:

$$\overline{u''} = \overline{f''} \overline{u'' \xi''} / \overline{f'' \xi''}. \quad (11)$$

This expression is very similar to the one early proposed by Jones (1994): $\overline{u''} = \overline{\xi''} \overline{u'' \xi''} / \overline{\xi''^2}$, but more general, i.e. suited to reactive flows. Moreover, for passive scalar mixing, i.e. $f = \xi$, Eq.(11) becomes strictly identical to Jones' expression.

Finally, the velocity splitting procedure provides algebraic and consistent closures for turbulent transport terms that account for thermal expansion effects. Their behaviour is in agreement with second order approach and it allows to recover and generalize available relations.

TURBULENT COMBUSTION MODEL

The final closure is obtained by considering the infinitely fast chemistry limit so that the turbulent flame brush corresponds to the chemical equilibrium, see Figure.(1). It must be noticed that this assumption has been retained for the sake of simplicity and the above model can be used as well with others flamelet closures. From a preliminary calculation of the chemical equilibrium, the mean density $\overline{\rho}$, mean temperature \overline{T} and mean species mass fractions can be tabulated from the mixture fraction Probability Density Function (PDF). A presumed β -PDF is considered here so that only the mean mixture fraction $\tilde{\xi}$ and its variance $\overline{\xi'^2}$ are required to define the PDF shape. Thus, only the

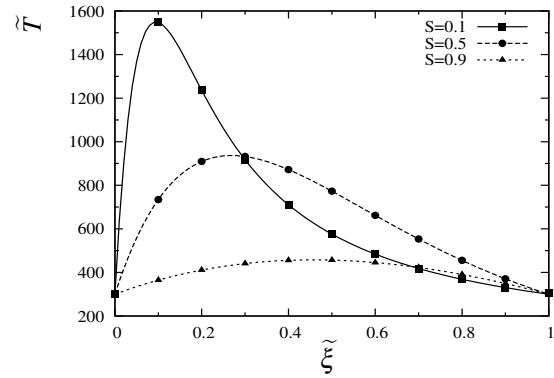


Figure 2: Temperature profiles obtained from tabulated data for three values of the segregation rate S .

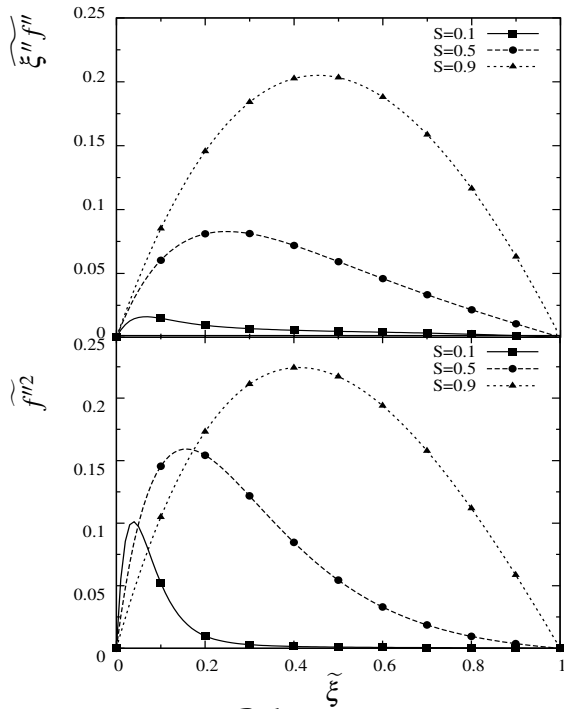


Figure 3: Correlation $\overline{\xi'' f''}$ profiles (top), and profiles of variance $\overline{f'^2}$ (bottom), as obtained from tabulated data for three values of the segregation rate S .

transport of these two averaged quantities is required to calculate the scalar fields. Figure (2) shows the profiles of mean temperature that can be obtained using such tabulated data for different values of the segregation rate, defined by $S = \overline{\xi'^2} / (\tilde{\xi}(1 - \tilde{\xi}))$. For small values of the segregation rate, the mean temperature profile approaches the chemical equilibrium profile presented in Fig.(1). However, for large values of the segregation rate the mean temperature is close to the fresh reactants temperature. These tabulated data also allow to determine the correlations involved in Eqs.(8-9-10), i.e $\overline{f'^2}$ and $\overline{\xi'' f''}$. Profiles of these quantities are reported in Fig.(3).

As expected for small levels of the segregation rate, these mean quantities reach a maximum close to the pure air side conditions. This behaviour can be associated with the strong variations of density around stoichiometric conditions, i.e. for low values of the mixture fraction, see Fig. 1. For large values of the segregation rate, the mixture is mainly composed of pure air and pure fuel pockets. Thus, profiles show a bimodal characteristic: parabolic shape with

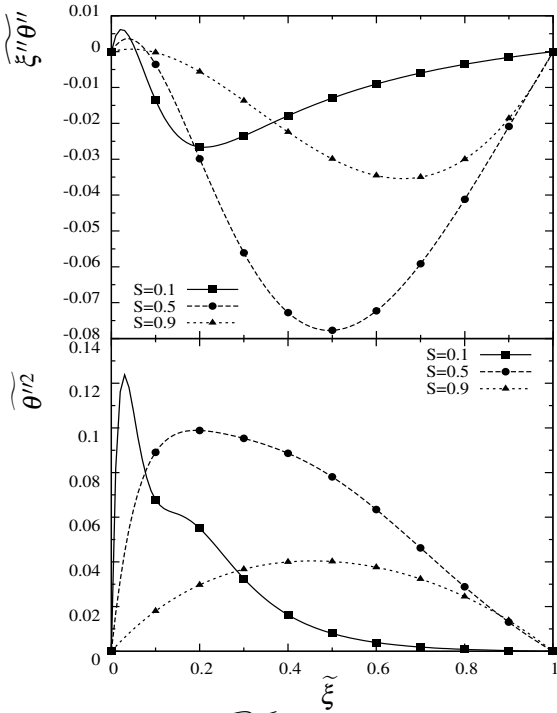


Figure 4: Correlation $\xi''\theta''$ profiles (top), and profiles of variance θ''^2 (bottom), as obtained from tabulated data for three values of the segregation rate S .

a maximum at $\xi = 0.5$. Accordingly, these correlations represent the effects of density variations induced by mixing but also by chemical reactions.

Now, to highlight the variable density effects that are only induced by chemical reactions, the same correlations are presented but the considered variable is a progress variable denoted θ , see Fig. (4). This progress variable is the normalized temperature defined as follows: $\theta = (T - T_{\min}) / (T_{\max} - T_{\min})$, where T_{\min} is the temperature of fresh reactants and T_{\max} the temperature at stoichiometry. The behaviour of the correlations profiles obtained with this reactive variable differs significantly from the one presented above in Fig.(3). For large values of the segregation rate, the correlations vanish because temperature in the two streams of fresh reactants are the same. For small values of the segregation rate, the progress variable variance θ''^2 exhibits the same behaviour as the variance f''^2 . However, the cross correlation $\theta''\xi''$ becomes negative in the main part of the flame brush whereas $f''\xi''$ is always positive. This result reflects the influence of the chemical equilibrium which leads to a maximum of the temperature profile $T(\xi)$ whereas the chemical equilibrium value of the specific volume $f(\xi)$ displays a monotonic evolution, see Fig. 1.

As our first objectives is to model the effects of chemical reactions on turbulent transports. We choose to consider the progress variable θ instead of the normalized specific volume f in Eqs. (8-9). Moreover, for the sake of simplicity, both model parameters λ and Ψ have been set to unity. The unit vector that characterizes the flux orientation of the second term of Eq. (8) have been defined as follows: $M = \nabla\theta / \|\nabla\theta\|$. Therefore, the final closure for the turbu-

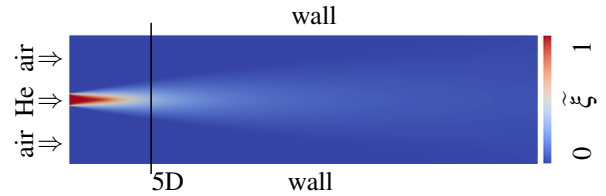


Figure 7: Studied configuration. Mean mixture fraction for non-reactive flow

lent transport terms writes:

$$\overline{\rho u'' \xi''} = -\overline{\rho}(\nu_T / \sigma_T) \nabla \xi + 2\overline{\rho} s \beta \xi'' \theta'' M. \quad (12)$$

$$\overline{\rho k} = \overline{\rho} k_{vT} + \overline{\rho} (s\beta)^2 \theta''^2. \quad (13)$$

The only unknown parameter in this set of equations is the chemical consumption rate s which should be related to the scalar dissipation rate (SDR). It can be obtained analytically in simplified cases, see for example Liñan & Crespo (1976); Marble & Broadwell (1977). It can be evaluated from detailed chemistry calculations as well. It must be pointed out that in the case of a stretched diffusion flame at the limit of extinction the value of s can be approximated as $s = \rho_{\max} S_L$, so that the proposed closure becomes fully consistent with the previous analysis conducted by Robin *et al.* (2011). In this study, we choose to express this chemical consumption rate as $s = \gamma \rho_{\max} S_L$, where γ is a model parameter. Whose sensitivity will be evaluated.

NUMERICAL SIMULATIONS OF INERT AND REACTIVE TURBULENT JETS

Density variations in hydrogen-air flames are due to both reactive and mixing processes and both may modify the scalar turbulent flux $\overline{\rho u'' \xi''}$ and turbulent kinetic energy $\overline{\rho k}$. However, the final closure proposed, i.e. Eqs. (12) and (13), is able to represent effects of density variations on turbulent fluxes induced by chemical reactions only. Thus, modifications of turbulent fluxes by the density variations induced by non reactive mixing are neglected. Therefore, we first checked that classical first order closures, for instance $k - \epsilon$ model and gradient law, are able to predict accurately enough the mean structure of the flow in an inert turbulent jet featuring large density variations, see Fig. 5 to Fig. 7. Indeed, the configuration considered is the jet of helium surrounded by a co-flow of air investigated by Djeridane *et al.* (1996) and Amielh *et al.* (1995). The numerical simulation is performed using the CFD code developed by eDF, Code_Saturne (Archambeau *et al.*, 2004). The mesh retained is made up of 10 000 cells.

Figure 7 shows the mean mixture fraction field obtained by the numerical simulation and the corresponding boundary conditions applied to the computational domain. The inlet boundary conditions have been taken from the data available in Djeridane *et al.* (1996) and Amielh *et al.* (1995). Results presented in Figs. 5 and 6 show a satisfactory agreement between the numerical simulation and experiments for the mean velocity, turbulent kinetic energy and mean mixture fraction.

These results confirm that the classical $k - \epsilon$ model associated with gradient law is able to predict the main structure of such an inert jet with variable density. Nevertheless, the density variations induced by combustion processes lead to local velocity variations that are expected to modify more

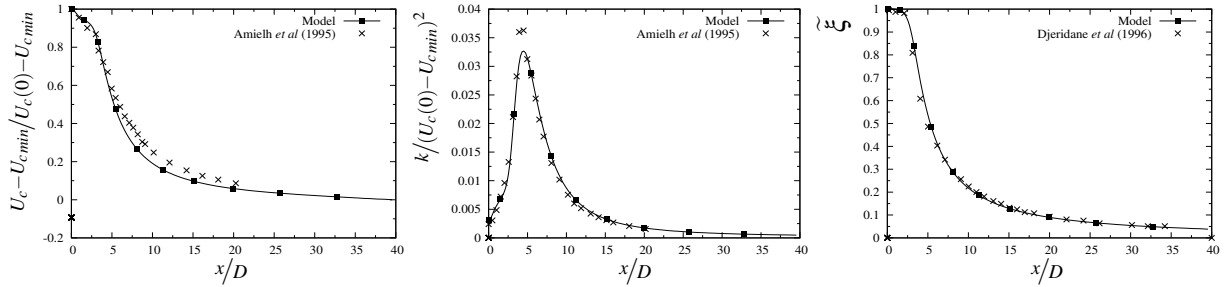


Figure 5: Axial distribution of normalized mean velocity, turbulent kinetic energy and mean mixture fraction for non-reactive flow with variable density.

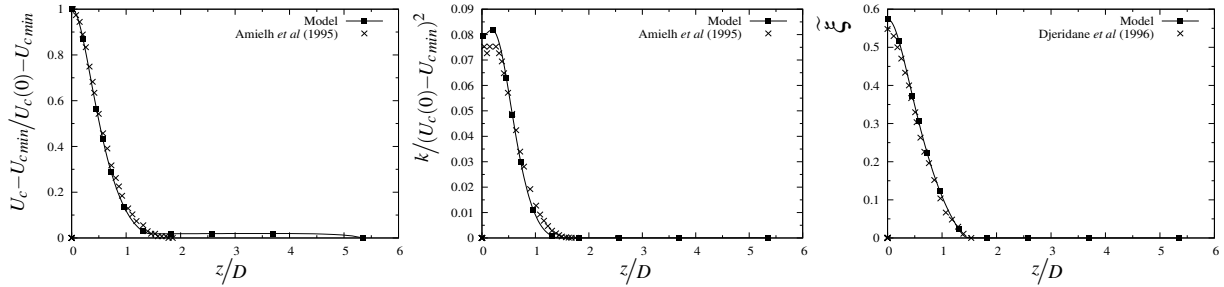


Figure 6: Radial distribution of normalized mean velocity, turbulent kinetic energy and mean mixture fraction for non-reactive flow with variable density located at $x/D = 5$.

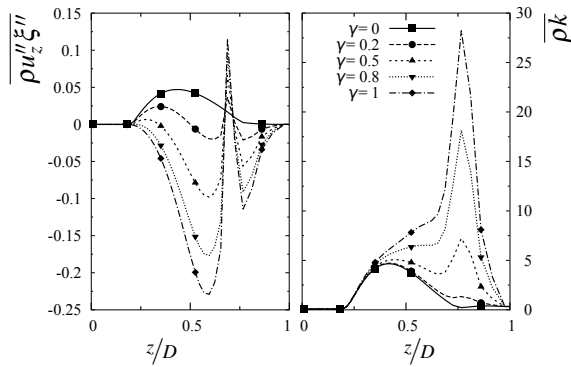


Figure 8: Transverse component of the scalar turbulent flux $\overline{\rho u_z'' \xi''}$ (left), turbulent kinetic energy $\overline{\rho k}$ (right), across the mean flame structure at $x = 5D$.

strongly turbulent fluxes and so the main structure of the flow. Accordingly, the closure proposed above, i.e. Eqs. (12) and (13), is now applied to the numerical simulation of a turbulent reactive jet of hydrogen surrounded by a co-flow of air, see for example Kent & Bilger (1973); Stårner & Bilger (1980); Kennedy & Kent (1981). The mesh retained is made up of 20 000 cells and the corresponding inlet boundary conditions have been taken from the data available in Kent & Bilger (1973). Fig. (8) shows the turbulent scalar flux $\overline{\rho u_z'' \xi''}$ and the turbulent kinetic energy $\overline{\rho k}$ obtained from numerical simulations along the radial direction z at $x/D = 5$. Profiles are also plotted versus the mean mixture fraction, see Fig. (9).

The sensitivity to the value of the parameter γ is evaluated. The case $\gamma = 0$ corresponds to the results obtained with a classical $k-\epsilon$ model associated with a gradient law and the case $\gamma = 1$ corresponds to the maximum chemical consumption rate that can be reached in such diffusion flames. Results clearly show that the scalar turbulent flux is strongly modified by thermal expansion even for small values of the chemical consumption rate, i.e. small values of γ . The scalar turbulent flux can even becomes negative, i.e.

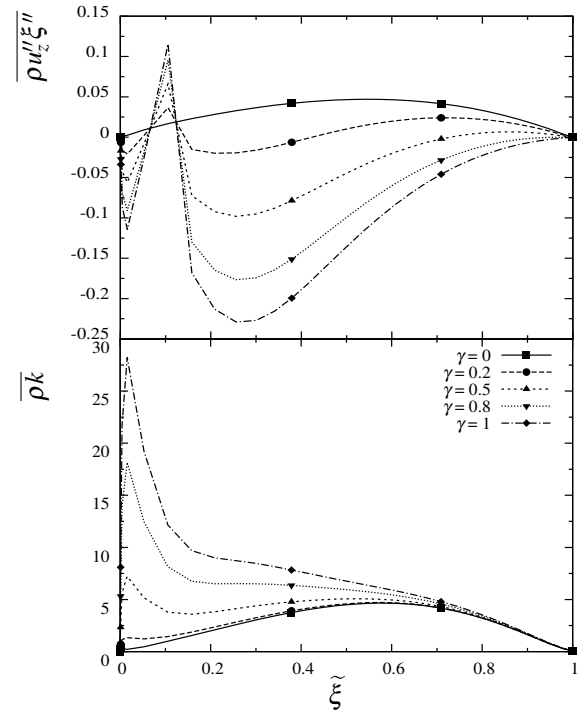


Figure 9: Transverse component of the scalar turbulent flux $\overline{\rho u_z'' \xi''}$ (top), Turbulent kinetic energy $\overline{\rho k}$ (bottom), across the mean flame structure at $x = 5D$ plotted versus the mean mixture fraction.

counter gradient, in the main part of the flame brush. however, the scalar turbulent flux is always found to be positive in a very narrow part of the flame brush near stoichiometric conditions. This peculiar behaviour is due to the changing signs of the correlation $\xi'' \theta''$ (see Fig. 4) and the changing direction of the unit vector $M = \nabla \theta / \|\nabla \theta\| = \nabla T / \|\nabla T\|$ (see Fig. 2) which both occur for small values of the mixture fraction. If the correlation $\xi'' \theta''$ reach zero at exactly the same location as the one associated with maximum tem-

perature value, then the thermal expansion effect on scalar turbulent flux vanishes at this location and is negative elsewhere enhancing the possible counter gradient turbulent diffusion effect. In other cases, the thermal expansion effect can be positive only in a very thin part of the flame brush enhancing, in this small area, the turbulent mixing processes. This behaviour is very similar to the one observed in premixed flame in the thin flame limit where the scalar turbulent flux is often counter gradient except in a very small region in front the flame brush. In turbulent diffusion flames, this region is found near stoichiometric conditions. It must be noticed that the scalar flux behaviour is partly controlled by the definition retained for the direction of the additional flux, i.e. the unit vector M . This direction may affect the value of the scalar flux component $\overline{\rho u'_z \xi''}$ but also its sign. We define M with the mean temperature gradient but other solutions could have been chosen. However, whatever the definition of M , an increase of turbulent kinetic energy will be observed, see Fig. 8. For small values of the mean mixture fraction, the turbulent kinetic energy can even be ten times higher when considering thermal expansion effects via Eq. (13). This phenomenon must be related to the correlation $\overline{\theta''^2}$ appearing in Eq. (13), see Figs. (9) and (4). Eventually, in turbulent diffusion flames, when the mixture fraction variance reach its maximum value ($S = 1$) or minimum value ($S = 0$), there is no effect of thermal expansion on turbulent fluxes. But for all intermediate values of the segregation factor, temperature fluctuations must lead to a strong production of turbulence. Moreover, considering large variations associated with very small values of the mixture fraction must lead to a change of behaviour in a very small region of the flame brush.

CONCLUSIONS

The description of hydrogen-air diffusion flame based on the mixture fraction as a passive scalar, the normalized temperature as a reactive scalar and the normalized specific volume allows to identify and treat separately density effects induced by both mixing and reactive processes. The closure strategy of turbulent transport terms is based on a velocity splitting procedure and leads to algebraic models for the turbulent scalar flux and the turbulent kinetic energy. These models allows to recover and generalise well-known previously established relations. The obtained expressions involve scalar variances and correlation that can be tabulated from chemical equilibrium or diffusion flamelets structures. The changing sign of the correlation must be directly related to the possible occurrence of counter-gradient diffusion. The calculation of practical turbulent diffusion hydrogen-air flame clearly shows a strong production of turbulence near stoichiometric conditions.

REFERENCES

- Amielh, M., Djeridane, T., Anselmet, F. & Fulachier, L. 1995 Velocity near-field of variable density turbulent jets. *Int. J. Heat Mass Transf.* **39** (10), 2149–2164.
- Archambeau, F., Mehitoua, N. & Sakiz, M. 2004 *Code Saturne: a finite volume code for turbulent flows. Int. J. Finite Volumes* **1**.
- Borghi, R. & Escudié, D. 1984 Assessment of a theoretical model of turbulent combustion by comparison with a simple experiment. *Combust. Flame* **56**, 149–164.
- Bray, K.N.C., Libby, P.A., Masuya, G.J. & Moss, J.B. 1981 Turbulence production in premixed turbulent flames. *Combust. Sci. Technol.* **25**, 127–140.
- Djeridane, T., Amielh, M., Anselmet, F. & Fulachier, L. 1996 Velocity turbulence properties in the nearfield region of axisymmetric variable density jets. *Phys. Fluids* **8** (6), 1614–1630.
- Dong, Q., Robin, V., Mura, A. & Champion, M. 2013 Analysis of algebraic closures of the mean scalar dissipation rate of the progress variable applied to stagnating turbulent flames. *Flow Turbulence Combustion* **90**, 301–323.
- Hardalupas, Y., Tagawa, M. & Taylor, A.M.K.P. 1996 Characteristics of countergradient heat transfer in non premixed swirling flame pp. 159–184.
- Jones, W.P. 1994 Turbulence modelling and numerical solution methods for variable density and combusting flows. In *Turbulent Reacting Flows* (ed. P. A Libby & F.A. Williams), pp. 309–374. Academic Press London.
- Kennedy, I.M. & Kent, J.H. 1981 Scalar measurements in a co-flowing turbulent diffusion flame. *Combust. Sci. Technol.* **25**, 109–119.
- Kent, J.H. & Bilger, R.W. 1973 Turbulent diffusion flames. *Proc. Combust. Inst.* **14** (1), 615 – 625.
- Libby, P.A. & Bray, K.N.C. 1981 Counter gradient diffusion in premixed turbulent flames. *AIAA J.* **19**, 205–213.
- Liñan, A. & Crespo, A. 1976 An asymptotic analysis of unsteady diffusion flames for large activation energies. *Combust. Sci. Technol.* **14**, 95–117.
- Luo, K.H. 2000 On local counter gradient diffusion in turbulent diffusion flames. *Proc. Combust. Inst.* **28**, 489–495.
- Luo, K.H. & Bray, K.N.C. 1998 Combustion induced pressure effects in supersonic diffusion flames. *Proc. Combust. Inst.* pp. 2165–2171.
- Marble, F.E. & Broadwell, J.E. 1977 The coherent flame model for turbulent chemical reactions. In *Project Squid Headquarters TRW-9-PU*. Chaffee Hall, Purdue University (USA).
- Robin, V., Mura, A. & Champion, M. 2011 Direct and indirect thermal expansion effects in turbulent premixed flames. *J. Fluid Mech.* **689**, 149–182.
- Robin, V., Mura, A. & Champion, M. 2012a Algebraic models for turbulent transports in premixed flames. *Combust. Sci. Technol.* **to appear**, DOI:10.1080/00102202.2012.690628.
- Robin, V., Mura, A. & Champion, M. 2012b A simple strategy to model the effects of thermal expansion on turbulent transports in premixed flames. *C. R. Acad. Sc. Mech. II soumis*.
- Stårner, S.H. 1983 Joint measurements of radial velocity and scalars in a turbulent diffusion flame. *Combust. Sci. Technol.* **30**, 145–169.
- Stårner, S.H. & Bilger, R.W. 1980 Lda measurements in a turbulent diffusion flame with axial pressure gradient. *Combust. Sci. Technol.* **21**, 259–276.
- Stårner, S.H. & Bilger, R.W. 1981 Measurements of scalar-velocity correlations in a turbulent diffusion flame. *Proc. Combust. Inst.* pp. 921–930.